

Search for solar axions produced by Compton process and bremsstrahlung using the resonant absorption and axioelectric effect

A.V. Derbin, I.S. Dratchnev, A.S. Kayunov, V.N. Muratova, D.A. Semenov, E.V. Unzhakov

St.Petersburg Nuclear Physics Institute, Gatchina, Russia 188300

DOI: will be assigned

The search for resonant absorption of Compton and bremsstrahlung solar axions by ^{169}Tm nuclei have been performed. Such an absorption should lead to the excitation of low-lying nuclear energy level: $A + ^{169}\text{Tm} \rightarrow ^{169}\text{Tm}^* \rightarrow ^{169}\text{Tm} + \gamma$ (8.41 keV). Additionally the axioelectric effect in silicon atoms is sought. The axions are detected using a Si(Li) detectors placed in a low-background setup. As a result, a new model independent restrictions on the axion-electron and the axion-nucleon coupling: $g_{Ae} \times |g_{AN}^0 + g_{AN}^3| \leq 2.1 \times 10^{-14}$ and the axion-electron coupling constant: $|g_{Ae}| \leq 2.2 \times 10^{-10}$ has been obtained. The limits leads to the bounds $m_A \leq 7.9$ eV and $m_A \leq 1.3$ keV for the mass of the axion in the DFSZ and KSVZ models, respectively (90% C.L.).

1 The axions spectra and the rate of axions resonant absorption by ^{169}Tm nucleus

If the axions or other axion-like pseudoscalar particles couple with electrons then they are emitted from Sun by the Compton process and by bremsstrahlung [1]-[6]. The expected spectrum of axions was calculated using theoretical predictions for the Compton cross section given in [7, 8] and the axion bremsstrahlung due to electron-nucleus collisions given in [9]. The axion flux is determined for radial distribution of the temperature, density of electrons and nuclei given by BS05(OP) Standard Solar Model [10] based on high-Z abundances [11]. The results of our calculations presented in Fig.1 [12].

As a pseudoscalar particle, the axion should be subject to resonant absorption and emission in the nuclear transitions of a magnetic type. In our experiment we have chosen the ^{169}Tm nucleus as a target. The energy of the first nuclear level ($3/2^+$) is equal to 8.41 keV, the total axion flux at this energy is $g_{Ae}^2 \times 1.34 \times 10^{33} \text{cm}^{-2} \text{s}^{-1} \text{keV}^{-1}$. The 8.41 keV nuclear level discharges through $M1$ -type transition with $E2$ -transition admixture value of $\delta^2 = 0.11\%$ and the relative probability of γ -ray emission is $\eta = 3.79 \times 10^{-3}$ [13].

The cross-section for the resonant absorption of the axions with energy E_A is given by the expression that is similar to the one for γ -ray resonant absorption, but the ratio of the nuclear transition probability with the emission of an axion (ω_A) to the probability of magnetic type transition (ω_γ) has to be taken into account [12]. The ω_A/ω_γ ratio calculated in the long-wave approximation, depends on isoscalar g_{AN}^0 and isovector g_{AN}^3 coupling constants and parameters

depending on the particular nuclear matrix elements [14, 15, 16].

As a result the rate of axion absorption by ^{169}Tm nucleus dependent only on the coupling constants is (the model-independent view) [12]:

$$R_A = 1.55 \times 10^5 g_{Ae}^2 (g_{AN}^0 + g_{AN}^3)^2 (p_A/p_\gamma)^3, \text{ s}^{-1}. \quad (1)$$

Using the relations between g_{AN}^0 , g_{AN}^3 and axion mass given by KSVZ model, the absorption rate can be presented as a function of g_{Ae} and axion mass m_A (m_A in eV units):

$$R_A = 5.79 \times 10^{-10} g_{Ae}^2 m_A^2 (p_A/p_\gamma)^3, \text{ s}^{-1}. \quad (2)$$

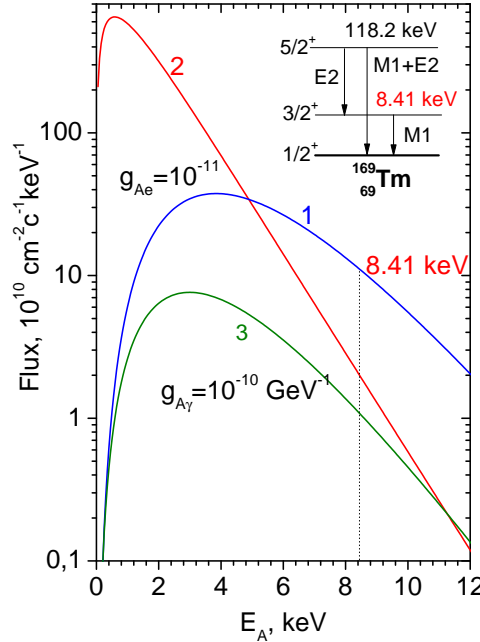


Figure 1: 1,2 - the spectra of the axions produced by the Compton process and the bremsstrahlung, correspondingly ($g_{Ae} = 10^{-11}$, $m_A = 0$) [12]. 3 - spectrum of the axions produced by Primakoff effect ($g_{A\gamma} = 10^{-10} \text{ GeV}^{-1}$). The level scheme of ^{169}Tm nucleus is shown in the inset [12].

2 Spectra of massive solar axions and a cross section for the axioelectric effect

If the mass of the axion is several keV, the expected solar axion spectra changes significantly and depends on the particular m_A value [19]. To calculate spectra we used the procedure similar described above. The spectra of solar axions were determined for different values of m_A [19].

An axion interacting with an electron should undergo axio-electric absorption, which is an analog of the photoelectric effect. Silicon atoms entering into the composition of a Si(Li) detector were used in our experiment as targets for the axio-electric effect. The cross section of the axioelectric absorption was calculated by the formula

$$\sigma_{abs}(E_A) = \sigma_{pe}(E_A) \frac{g_{Ae}^2}{\beta} \frac{3E_A^2}{16\pi\alpha m_e^2} \left(1 - \frac{\beta}{3}\right) \quad (3)$$

where σ_{pe} is the cross section for the photoelectric effect and $\beta = v/c = p_A/E_A$ is the velocity of the axion. At $\beta \rightarrow 1$ and $\beta \rightarrow 0$, this formula coincides with the cross sections for relativistic and nonrelativistic axions obtained in [17, 18] and provides an extrapolation approximately linear in β , which ensures a sufficient accuracy for the case under consideration.

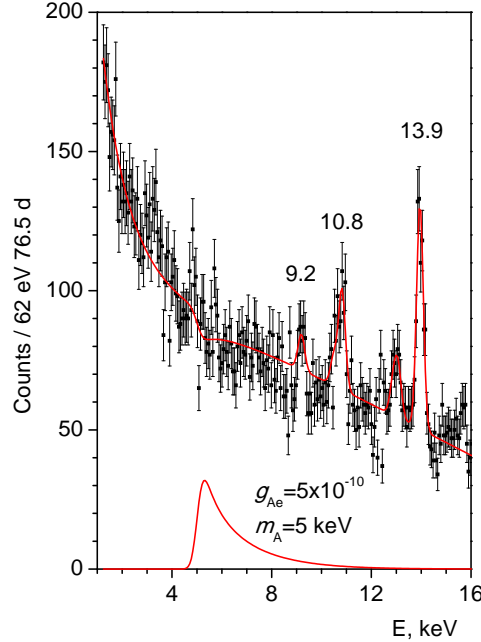


Figure 2: Spectrum of the signals of the Si(Li) detector in the range of (1–16) keV with the optimal fit for $m_A = 5$ keV. The energies of the Gaussian peaks are given near them. The expected spectrum is shown for the case of the detection of axions with $m_A = 5$ keV and $g_{Ae} = 5 \times 10^{-10}$.

The expected signal from 5 keV axions undergoing axioelectric effect in Si-detector is shown in Fig.2.

3 Experimental setups

To search for quanta with an energy of 8.41keV due to axion resonant absorption, the planar Si(Li) detector with a sensitive area diameter of 66 mm and a thickness of 5 mm was used.

The detector was mounted on 5 cm thick copper plate that protected the detector from the external radioactivity. The detector and the holder were placed in a vacuum cryostat and cooled to liquid nitrogen temperatures. A Tm_2O_3 target of 2 g mass was uniformly deposited on a plexiglas substrate 70 mm in diameter at a distance of 1.5 mm from the detector surface. External passive shielding composed of copper, iron and lead layers was adjusted to the cryostat and eliminated external radioactivity background by a factor of about 500.

To search for axioelectric effect we used a Si(Li) detector with a sensitive-region diameter of 17 mm and a thickness of 2.5 mm. The detector was placed in a vacuum cryostat with the input beryllium window 20 μm thick. The window was used for energy calibration and determination of the detection efficiency of gamma-ray photons in order to find the sensitive volume of the detector. The detector was surrounded by 12.5 cm of copper and 2.5 cm of lead, which reduced the background of the detector at an energy of 14 keV by a factor of 110 as compared to the unshielded detector.

The experimental setups were located on the ground surface. Events produced by cosmic rays and fast neutrons were registered by an active shielding consisting of five plastic scintillators $50 \times 50 \times 12$ cm in size. The rate of 50 μs veto signals was 600 counts/s, that lead to $\approx 3\%$ dead time. More details of experiments one can find in [12, 19].

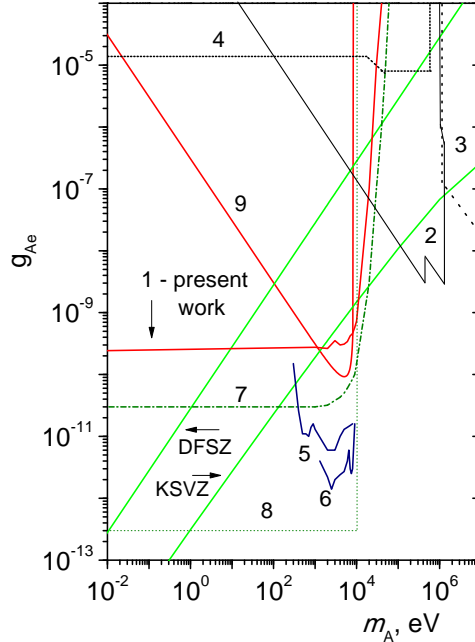


Figure 3: Bounds for the axion-electron coupling constant: (1) Si-axioelectrical effect [19], (2) reactor experiments and solar axions with energies of 0.478 and 5.5 MeV,(3) beam dump experiments, (4) decay of orthopositronium, (5) CoGeNT, (6) CDMS, (7) bound for the axion luminosity of the Sun, (8) red giants and (9) experiment with ^{169}Tm . The regions of excluded values lie above the corresponding lines. The inclined lines show the g_{Ae} values in the DFSZ and KSVZ ($E/N = 8/3$) models.

4 Results

The upper limit on axions absorption rate by ^{169}Tm nucleus $R_A \leq 5.43 \times 10^{-23}\text{s}^{-1}$ set by our experiment limits the possible values of coupling constants g_{Ae} , g_{AN} and axion mass m_A . According to (1) and (2) and taking into account the approximate equality of the axion and γ -quantum momenta $(p_A/p_\gamma)^3 \simeq 1$ for $m_A \leq 2$ keV we obtain (at 90% c.l.):

$$g_{Ae} \times |(g_{AN}^0 + g_{AN}^3)| \leq 2.1 \times 10^{-14} \quad (4)$$

$$g_{Ae} \times m_A \leq 3.1 \times 10^{-7} \text{ eV} \quad (5)$$

The restriction (4) is a model independent one on axion (or any other pseudoscalar particle) couplings with electron and nucleons. The result (5) presented as a restriction on the range of possible values of g_{Ae} and m_A (KSVZ relations between g_{AN} and m_A are used) allows one to compare our result (Fig.3, line 9) with results of other experiments restricting g_{Ae} (Fig.3). The limits on $g_{Ae} \times m_A$ for DFSZ axion lie in the range $(0.33 - 1.32)$ of the restriction. As we mention in [20, 12] the sensitivity of experiment with ^{169}Tm can be increased significantly (in $\sim 10^6$ times) by introducing the Tm target inside the sensitive volume of detector having high energy resolution, at present, cryogenic detectors have the best option.

When looking for the axioelectric effect the measured spectrum is fitted by the sum of an exponential function, describing the smooth background and the response function for axions $S(E, m_A)$:

$$N(E) = a + b \exp(cE) + g_{Ae}^4 S(E, m_A) N_{Si} T \quad (6)$$

Here, N_{Si} is the number of silicon atoms in the sensitive volume of the detector and $T = 6.61 \times 10^6$ is the live time of measurement. The upper bound for $|g_{Ae}|$ at $m_A=0$ is

$$|g_{Ae}| \leq 2.2 \times 10^{-10} \quad (7)$$

at 90% C.L. Limit (7) is a model independent bound for the coupling constant of the axion or any other pseudoscalar relativistic particle with the electron.

For nonrelativistic axions the fitting range was expanded to 16 keV. To describe the experimental spectrum in a wide range, function 6 was supplemented by a linear term for describing the continuous background and six Gaussians for describing the peaks of the characteristic Np X rays manifested in the measurements [20, 21]. The fit results and $S(E, m_A)$ for $m_A = 5$ keV are shown in Fig.2.

The maximum deviation of g_{Ae}^4 from zero for all tested (from 1 to 10 keV with a step of 1 keV) m_A values is 2.5σ . The upper bounds obtained for $|g_{Ae}|$ at various m_A values are shown in Fig.3 (line 1) in comparison with the other experimental results.

5 Acknowledgments

This work was supported by RFBR grants 13-02-01199-a and 13-02-12140-ofi-m.

References

- [1] K. Kato, H. Sato, Prog. Theor. Phys. **54**, 1564 (1975)
- [2] M.I. Vysotsskii, Ya.B. Zeldovich, M.Yu. Khlopov, V.M. Chechetkin, JETP Lett. **27**, 502 (1978)

- [3] D.A. Dicus, E.W. Colb, V.L. Teplitz, R.V. Wagover, Phys. Rev. D **18**, 1829 (1978), D **22**, 839 (1980)
- [4] M. Fukugita, S. Watamura, M. Yoshimura, Phys. Rev. Lett. **48**, 1522 (1982)
- [5] L.M. Krauss, J.E. Moody, F. Wilczek, Phys. Lett. B **144**, 391 (1984)
- [6] G.G. Raffelt, Phys. Rev. D **33**, 897 (1986)
- [7] M. Pospelov, A. Ritz and M.B. Voloshin, Phys. Rev. D **78**, 115012 (2008) [arXiv:0807.3279]
- [8] P. Gondolo and G.G. Raffelt Phys. Rev. D **79**, 107301 (2009) [arXiv:0807.2926]
- [9] A.R. Zhitnitsky, Yu.I. Skovpen, Sov. J. Nucl. Phys. **29**, 513 (1979)
- [10] J.N. Bahcall, A.M. Serenelli, and S. Basu, Astrophys. J. **621**, L85 (2005)
- [11] M. Asplund, N. Grevesse, and J. Sauval, Nucl. Phys. A **777**, 1 (2006)
- [12] A.V. Derbin *et al.* Phys. Rev. D **83**, 023505 (2011) [arXiv:1101.2290]
- [13] C.M. Baglin, Nucl. Data Sheets, **109**, 2033 (2008)
- [14] T.W. Donnelly *et al.* Phys. Rev. D **18**, 1607 (1978)
- [15] F.T. Avignone III *et al.* Phys. Rev. D **37**, 618 (1988)
- [16] W.C. Haxton and K.Y. Lee, Phys. Rev. Lett. **66**, 2557 (1991)
- [17] M. Pospelov, A. Ritz, and M.B. Voloshin, Phys. Rev. D **78**, 115012 (2008)
- [18] A. Derevianko *et al.* Phys. Rev. D **82**, 065006 (2010)
- [19] A.V. Derbin, I.S. Drachnev, A.S. Kayunov, V.N. Muratova, JETP Lett. **95**, 379 (2012) [arXiv:1206.4142]
- [20] A.V. Derbin *et al.* Phys. Lett. B **678**, 181 (2009) [arXiv:0904.3443]
- [21] A.V. Derbin *et al.* Eur. Phys. J. C **62**, 755 (2009) [arXiv:0906.0256]